SUPPLEMENTAL MATERIAL

Table 1. Patient Exclusions

	Training (Baylor)	Validation (MSKCC)
Total Patients Received	539	366
Total Patients Analyzed	262	61
Reason for Removal[a]		
PSA Outcome Missing	30	0
PSA Never Became Undetectable	Not Collected	34
Received Neoadjuvant Therapy	3	0
Received Adjuvant Therapy	7	1
Biomarker Information Missing	52	42
Insufficient Tumor Content in H&E Image	271	301

[a]Some patients had more than one reason for removal.

Table 2. Original Study Clinical and Pathologic Information

	Training		Validation	
Characteristic	**Full Cohort**	**Evaluable**	**Full Cohort**	**Evaluable**
N	539	262	366	61
Age (years)				
Mean	62	62	61	61
Median	63	63	61	62
Range	38–86	38–81	42–77	42–74
Race				
Caucasian	479 (88.9%)	235 (89.7%)	339 (92.6%)	58 (95.1%)
African-American (Hispanic and Non-Hispanic)	31 (5.8%)	21 (8.0%)	15 (4.1%)	2 (3.3%)
Other/Unknown	29 (5.4%)	6 (2.3%)	12 (3.3%)	1 (1.6%
Pre-operative PSA (ng/mL)				
Mean	9.8	10.7	10.7	12.9
Median	7.3	7.8	8.0	10.0
Range	0.2–82.0	0.9–81.9	0.6–69.5	2.0–69.5
Pathologic TNM Stage				
T2N0	322 (62.2%)	158 (60.3%)	Not Collected	Not Collected
T3aN0	128 (24.7%)	70 (26.7%)	Not Collected	Not Collected
T3bN0	41 (7.9%)	17 (6.5%)	Not Collected	Not Collected
T1-3N+	27 (5.2%)	17 (6.5%)	Not Collected	Not Collected
Missing	21	0	Not Collected	Not Collected
UICC Stage				
T1a < 5%	1 (0.2%)	1 (0.4%)	Not Collected	Not Collected
T1b ≥ 5%	5 (1.2%)	1 (0.4%)	Not Collected	Not Collected
T1c not palpable or visible	187 (43.7%)	113 (43.1%)	Not Collected	Not Collected
T2a ≤ ½ lobe	88 (20.6%)	54 (20.7%)	Not Collected	Not Collected
T2b ≤ 1 lobe	72 (16.8%)	43 (16.4%)	Not Collected	Not Collected
T2c both lobes	53 (12.4%)	33 (12.6%)	Not Collected	Not Collected
T3a unilateral ECE	19 (4.4%)	15 (5.7%)	Not Collected	Not Collected
T3c SV+	3 (0.7%)	2 (0.8%)	Not Collected	Not Collected
Missing	111	0	Not Collected	Not Collected
Digital Rectal Exam Result				
Non-palpable	235 (47.9%)	122 (46.6%)	187 (51.1%)	32 (52.5%)
Palpable	256 (52.1%)	140 (53.4%)	179 (48.9%)	29 (47.5%)
Missing	48	0	0	0
Lymph Node Involvement				
Negative	492 (94.8%)	246 (93.9%)	343 (93.7%)	56 (91.8%)
Positive	27 (5.2%)	16 (6.1%)	23 (6.3%)	5 (8.2%)
Missing	20	0	0	0
Seminal Vesicle Involvement				
No	480 (89.2%)	233 (88.9%)	315 (86.1%)	51 (83.6%)
Yes	58 (10.8%)	29 (11.1%)	51 (13.9%)	10 (16.4%)
Missing	1	0	0	0
Surgical Margins				
Negative	448 (83.1%)	216 (82.4%)	238 (65.0%)	36 (59.0%)
Positive	91 (16.9%)	46 (17.6%)	128 (35.0%)	25 (41.0%)
Extracapsular Involvement				
No	338 (65.0%)	159 (60.7%)	253 (69.1%)	43 (70.5%)
Yes	182 (35.0%)	103 (39.3%)	113 (30.9%)	18 (29.5%)
Missing	19	0	0	0
Dominant Biopsy Gleason Grade				
1	3 (0.6%)	1 (0.4%)	1 (0.3%)	0 (0.0%)
2	92 (18.6%)	43 (16.4%)	5 (1.4%)	0 (0.0%)
3	336 (67.9%)	181 (69.1%)	283 (77.3%)	39 (63.9%)

Characteristic	Training		Validation	
	Full Cohort	Evaluable	Full Cohort	Evaluable
4	62 (12.5%)	36 (13.7%)	77 (21.0%)	22 (36.1%)
5	2 (0.4%)	1 (0.4%)	0 (0.0%)	0 (0.0%)
Missing	44	0	0	0
Biopsy Gleason Score				
2	1 (0.2%)	1 (0.4%)	1 (0.3%)	0 (0.0%)
3	3 (0.6%)	0 (0.0%)	0 (0.0%)	0 (0.0%)
4	21 (4.2%)	7 (2.7%)	4 (1.1%)	0 (0.0%)
5	112 (22.6%)	56 (21.4%)	10 (10.0%)	3 (4.9%)
6	197 (39.8%)	97 (37.0%)	209 (57.1%)	27 (44.3%)
7	135 (27.3%)	85 (32.4%)	110 (30.1%)	20 (32.8%)
8	22 (4.4%)	13 (5.0%)	23 (6.3%)	8 (13.1%)
9	4 (0.8%)	3 (1.2%)	9 (2.5%)	3 (4.9%)
Missing	44	0	0	0
Dominant Specimen Gleason Grade				
2	49 (9.1%)	20 (7.6%)	1 (0.3%)	0 (0.0%)
3	410 (76.1%)	198 (75.6%)	265 (72.4%)	34 (55.7%)
4	78 (14.5%)	44 (16.8%)	95 (26.0%)	23 (37.7%)
5	2 (0.4%)	0 (0.0%)	5 (1.4%)	4 (6.6%)
Specimen Gleason Score				
5	51 (9.5%)	21 (8.0%)	3 (0.8%)	1 (1.6%)
6	198 (36.7%)	86 (32.8%)	102 (27.9%)	8 (13.1%)
7	263 (48.8%)	144 (55.0%)	213 (58.2%)	37 (60.7%)
8	23 (4.3%)	11 (4.2%)	25 (6.8%)	7 (11.5%)
9	4 (0.7%)	0 (0.0%)	23 (6.3%)	8 (13.1%)
Ploidy				
Diploid	295 (54.7%)	141 (53.8%)	Not Collected	Not Collected
Tetraploid	219 (40.6%)	113 (43.1%)	Not Collected	Not Collected
Aneuploid	15 (2.8%)	8 (3.1%)	Not Collected	Not Collected
Missing	10 (1.9%)	0 (0.0%)	Not Collected	Not Collected
Percent Ploidy in S Phase (%)				
Mean	2.6	2.4	Not Collected	Not Collected
Median	1.3	1.2	Not Collected	Not Collected
Range	0.0 – 66.4	0.0 – 66.4	Not Collected	Not Collected
Percent Ploidy Fraction				
Mean	3.7	3.4	Not Collected	Not Collected
Median	2.5	2.4	Not Collected	Not Collected
Range	0.0– 20.0	0.0–20.0	Not Collected	Not Collected

Table 3. Extended Study Clinical and Pathologic Information

Characteristic	Training	Validation
N	342	340
Pre-operative PSA (ng/mL)		
Mean	10.3	10.8
Median	7.5	7.9
Range	0.8–68.5	1.01–100.0
Lymph Node Involvement		
Negative	339 (99.1%)	335 (98.5%)
Positive	3 (0. 9%)	5 (1.5%)
Seminal Vesicle Involvement		
No	320 (93.6%)	321 (94.4%)
Yes	22 (6.4%)	19 (5.6%)

Characteristic	Training	Validation
Surgical Margins		
Negative	219 (64.0%)	240 (71.0%)
Positive	123 (36.0%)	100 (29.0%)
Extracapsular Involvement		
No	245 (71.6.0%)	254 (74.7%)
Yes	97 (28.4%)	86 (25.3%)
Dominant Biopsy Gleason Grade		
1	1 (0.3%)	2 (0.6%)
2	17 (5.0%)	23 (6.8%)
3	279 (81.6%)	273 (80.3%)
4	45 (13.2%)	42 (12.4%)
5	0 (0.0%)	0 (0.0%)
Biopsy Gleason Score		
2	0 (0.0%)	1 (0.3%)
3	1 (0.3%)	2 (0.6%)
4	11 (3.2%)	8 (2.4%)
5	23 (6.7%)	30 (8.8%)
6	190 (55.6%)	187 (55.0%)
7	101 (29.5%)	94 (27.7%)
8	15 (4.4%)	13 (3.8%)
9	1 (0.3%)	5 (1.5%)
Dominant Specimen Gleason Grade		
2	8 (2.3%)	5 (1.5%)
3	283 (82.8%)	276 (81.2%)
4	49 (14.3%)	55 (16.2%)
5	2 (0.6%)	4 (1.2%)
Specimen Gleason Score		
5	9 (2.6%)	15 (4.4%)
6	116 (33.9%)	110 (32.4%)
7	193 (56.4%)	187 (55.0%)
8	18 (5.3%)	17 (5.0%)
9	6 (1.8%)	10 (2.9%)
10	0 (0.0%)	1 (0.3%)

Table 4. Imaging Features

Feature Name	Description
CytoplasmMeanMeanChannel40058	Mean of cytoplasm intensity mean value with the red filter
CytoplasmMeanMeanChannel50059	Mean of cytoplasm intensity mean value with the green filter
CytoplasmMeanMeanChannel60060	Mean of cytoplasm intensity mean value with the blue filter
CytoplasmMeanStddevChannel40066	Mean of cytoplasm intensity standard deviation with the red filter
CytoplasmMeanStddevChannel50067	Mean of cytoplasm intensity standard deviation with the green filter
CytoplasmMeanStddevChannel60068	Mean of cytoplasm intensity standard deviation with the blue filter
CytoplasmStddevMeanChannel40081	Standard deviation of the mean cytoplasm intensity with the red filter
CytoplasmStddevMeanChannel50082	Standard deviation of the mean cytoplasm intensity with the green filter
CytoplasmStddevMeanChannel60083	Standard deviation of the mean cytoplasm intensity with the blue filter
EpithelNucleiMeanMeanChanne40112	Mean of epithelial nuclei intensity with the red filter
EpithelNucleiMeanMeanChanne50113	Mean of epithelial nuclei intensity with the green filter
EpithelNucleiMeanMeanChanne60114	Mean of epithelial nuclei intensity with the blue filter
EpitheNucleiMeanStddevChann40120	Mean of epithelial nuclei intensity standard deviation with the red filter
EpitheNucleiMeanStddevChann50121	Mean of epithelial nuclei intensity standard deviation with the green filter
EpitheNucleiMeanStddevChann60122	Mean of epithelial nuclei intensity standard deviation with the blue filter
EpitheliaNucleiStddevAreaPxl0124	Standard deviation of the epithelial nuclei area
EpitheNucleiStddevMeanChann40135	Standard deviation of the mean epithelial nuclei intensity with the red filter
EpitheNucleiStddevMeanChann50136	Standard deviation of the mean epithelial nuclei intensity with the green filter
EpitheNucleiStddevMeanChann60137	Standard deviation of the mean epithelial nuclei intensity with the blue filter
StromaMeanMeanChannel40262	Mean of stroma intensity with the red filter
StromaMeanMeanChannel50263	Mean of stroma intensity with the green filter
StromaMeanMeanChannel60264	Mean of stroma intensity with the blue filter
StromaMeanStddevChannel40270	Mean of stroma intensity standard deviation with the red filter
StromaMeanStddevChannel50271	Mean of stroma intensity standard deviation with the green filter
StromaMeanStddevChannel60272	Mean of stroma intensity standard deviation with the blue filter
StromaStddevMeanChannel40331	Standard deviation of the mean stroma intensity with the red filter
StromaStddevMeanChannel50332	Standard deviation of the mean stroma intensity with the green filter
StromaStddevMeanChannel60333	Standard deviation of the stroma intensity with the blue filter
AreaCytopdivTotTissueArea	Area of cytoplasm relative to the tissue area, %
AreaEpitNucdivTotTissueArea	Area of epithelial nuclei relative to the tissue area, %
AreaLumendivTotTissueArea	Area of lumen relative to the tissue area, %
AreaRBCdivTotTissueArea	Area of red blood cells relative to the tissue area, %
AreaStromadivTotTissueArea	Area of stroma relative to the tissue area, %

Table 5. Molecular Features

Feature	Description
atki67t1	Tumor Ki-67 1
atki67t2	Tumor Ki-67 2
atki67t3	Tumor Ki-67 3
atki67p1	PIN Ki-67 1
atki67p2	PIN Ki-67 2
atki67p3	PIN Ki-67 3
atki67a1	Atrophic Gland Ki-67 1
atki67a2	Atrophic Gland Ki-67 2
atki67a3	Atrophic Gland Ki-67 3
atc18t3	Tumor Cytokeratin18
atcd45t3	Tumor CD45
atcd68t3	Tumor CD68
atcd34p	CD34 (adjacent to PIN)
atcd34s	CD34 (in stroma)
atcd34t	CD34 (adjacent to tumor)
atcd34tp	CD34 (adjacent to(tumor and PIN)
atcd34ts	CD34 (adjacent to tumor and in stroma)
atcd34ps	CD34 (adjacent to PIN and in stroma)
atc18p3	PIN with Cytokeratin 18
atcd45p3	CD45 associated with PIN
atc18a3	Atrophic Gland with Cytokeratin 18
atcd45a3	CD45 associated with Atrophic Gland
arsi	Tumor AR staining index
c14si	Tumor Cytokeratin 14 staining index
cd1si	Tumor Cyclin D1 staining index
psasi	Tumor PSA staining index
psmasi	Tumor PSMA staining index
p27si	Tumor $p27^{Kip1}$ staining index
her2si	Tumor Her-2/neu staining index
arpsi	PIN AR staining index
c14psi	PIN Cytokeratin 14 staining index
cd1psi	PIN Cyclin D1 staining index
psapsi	PIN PSA staining index
psmapsi	PIN PSMA staining index
p27psi	PIN $p27^{Kip1}$ staining index
her2psi	PIN Her-2/neu staining index
arasi	Atrophic Gland AR staining index
c14asi	Atrophic Gland Cytokeratin 14 staining index
cd1asi	Atrophic Gland Cyclin D1 staining index
psaasi	Atrophic Gland PSA staining index
psmaasi	Atrophic Gland PSMA staining index
p27asi	Atrophic Gland $p27^{Kip1}$ staining index
her2asi	Atrophic Gland Her-2/neu staining index

Table 6a. Percentage of Cells Staining, by Histologic Component and Staining Intensity (Training Set)

	Tumor			PIN			Atro	
Marker	**1+**	**2+**	**3+**	**1+**	**2+**	**3+**	**1+**	
Ki-67								
Mean ± SD	22.0 ± 30.4	7.2 ± 17.1	1.8 ± 4.0	23.0 ± 31.5	7.8 ± 18.3	2.0 ± 4.5	1.3 ± 8.05	1
Median	0.7	0.0	0.0	1.0	0.0	0.0	0.0	0
Range	0.0–100.0	0.0–100.0	0.0–26.3	0.0–100.0	0.0–100.0	0.0–39.5	0.0–96.0	0
CK18								
Mean ± SD	NA	NA	100.0 ± 0.04	NA	NA	100.0 ± 0.04	NA	
Median	NA	NA	100.0	NA	NA	100.0	NA	
Range	NA	NA	50.0–100.0	NA	NA	50.0–100.0	NA	
CD45								
Mean ± SD	NA	NA	0.0 ± 0.04	NA	NA	0.0 ± 0.01	NA	
Median	NA	NA	0.0	NA	NA	0.0	NA	
Range	NA	NA	0.0–0.4	NA	NA	0.0–0.1	NA	
CD68								
Mean ± SD	NA	NA	0.0 ± 0.01	NA	NA	NA	NA	
Median	NA	NA	0.0	NA	NA	NA	NA	
Range	NA	NA	0.0–0.1	NA	NA	NA	NA	

Table 6b. Staining Index by Histologic Component (Training Set)

Marker	Tumor	PIN	Gland
AR			
Mean ± SD	171.8 ± 75.9	79.9 ± 83.3	29.5 ± 67.9
Median	200	66.0	0
Range	0–300	0–300	0–300
CK14			
Mean ± SD	2.2 ± 6.4	35.2 ± 62.0	8.3 ± 32.6
Median	0	0	0
Range	0–69	0–300	0–300
Cyclin D1			
Mean ± SD	1.4 ± 7.1	0.0 ± 0.21	0.0 ± 0.0
Median	0	0	0
Range	0–90	0–3	0–0
PSA			
Mean ± SD	117.9 ± 71.2	140.5 ± 97.4	22.4 ± 54.9
Median	100	134	0
Range	0–300	0–300	0–300
PSMA			
Mean ± SD	0.3 ± 2.1	5.8 ± 19.8	3.0 ± 23.2
Median	0	0	0
Range	0–21	0–154	0–300
$p27^{Kip1}$			
Mean ± SD	3.9 ± 8.2	6.6 ± 19.0	1.3 ± 8.7
Median	0	0	0
Range	0–48	0–140	0–120
Her-2/neu			
Mean ± SD	3.5 ± 16.9	0.2 ± 1.1	0.0 ± 0.0
Median	0	0	0
Range	0–150	0–10	0–0

Table 6c. Percentage of Cells with CD34 Staining, by Histologic Component (Training)

	PIN	Stroma	Tumor	Tumor/PIN	Tumor/Stroma	PIN/Stroma
Mean ± SD	0.0 ± 0.04	0.0 ± 0.11	0.1 ± 0.18	0.0 ± 0.07	0.0 ± 0.08	0.0 ± 0.04
Median	0.0	0.0	0.0	0.0	0.0	0.0
Range	0.0–0.4	0.0–1.7	0.0–0.9	0.0–0.5	0.0–0.4	0.0–0.3

Table 7. Immunofluorescent Quantitative Androgen Receptor Features Derived from Histologic Labeling Tool software.

Feature	Definition
averageip0001	Average Intensity of AR in epithelial nuclei
averageip0002	Average Intensity of AR in all nuclei
averageipstroma0003	Average Intensity of AR in stromal nuclei
indexp0004	Min-Max average of AR in epithelial nuclei
indexp0005	Mix-Max average of AR in all nuclei
indexpstroma0006	Min-Max average of AR in stromal nuclei
maxip0007	Max AR in epithelial nuclei
maxip0008	Max AR in all nuclei
maxipstroma0009	Max AR in stromal nuclei
minip0010	Min AR in epithelial nuclei
minip0011	Min AR in all nuclei
minipstroma0012	Min AR in stromal nuclei
ratioareaepithnucversusepith0013	AR+ epithelial nuclei / AR- epithelial nuclei
backgroundi0001	Background
dapiwithar0002	AR- nuclei
dapiwithar0003	AR+ nuclei
eoi0004	Element of Interest
correlaobject10005	DAPI and AR correlation

Methods

Image Analysis and Morphometry

For tissue segmentation, image objects were classified into histopathological classes using spectral characteristics, shape characteristics, and spatial relationships between tissue histopathological objects. The H&E image scripts were developed to extract features from selected patient images. Given the heterogeneity of prostate cancer in association with benign elements, we trained our initial scripts on images which contained an abundance (>80%) tumor content. We subsequently reduced the amount of required tumor content in the validation cohort to 50% or greater in order to maximize the number of patients included in the analysis. For the expanded study we used Adobe Imageready 7.0 to digitally outline and color-mask infiltrative tumor-only regions within individual cores for subsequent image processing. The following histopathological objects were analyzed. "Background" is the portion of the digital image that is not occupied by tissue. "Cytoplasm" is the amorphous pink area that surrounds an epithelial nucleus and does not refer to the stromal cytoplasm. "Epithelial nuclei" are round objects surrounded by cytoplasm. "Lumen" is an enclosed white area surrounded by epithelial cells. Occasionally, the lumen can be filled by prostatic fluid (pink) or other "debris" (e.g., macrophages, dead cells, etc.). Together the lumen and the epithelial nuclei form a gland unit. The area between gland units is occupied by stroma which consists of connective tissue (i.e. fibroblasts, myofibroblasts, blood vessels) with contains a variable density that maintains the architecture of the prostatic tissue. "Stroma nuclei" are elongated cells with minimal amounts of cytoplasm (fibroblasts). This stromal category includes endothelial cells and inflammatory cells, while epithelial nuclei may be found

scattered within the stroma if infiltrative prostate cancer is present within the image. "Red blood cells" are small red round objects usually located within the vessels (arteries or veins), but can also be found dispersed throughout tissue. Artifact refers to fissures and 'cracks' within the section as a result of dehydration and fixation during processing of the tissue sample and does not reflect a true histologic structure within the prostate tissue sample under evaluation.

For a given histopathological object, its properties were computed and output as morphometric features. Properties included both spectral properties (color channel values, standard deviations, and brightness (across all channels) and generic shape properties (area, length, width, compactness, density, etc). Statistics (minimum, maximum, mean, and standard deviation) were computed for each property specific to a histopathologic object.

Immunohistochemical Analysis:

Antigen retrieval was performed by incubation with a 0.01 M citrate buffer (pH 6) for 30 min in a pressure cooker. Primary antibodies (Supplementary Table 7) were diluted in PBS with 0.1% sodium azide and applied for 16 h at 4 C followed by biotinylated secondary antibodies (Vector) at 1:1000 dilution for 1 h. Negative control slides received normal mouse serum (DAKO) as the primary antibody. Slides were counterstained with Harris Hematoxylin and the staining patterns of the individual antibodies were scored independently by two pathologists (AK, MJD) with all discrepancies resolved by a third pathologist (CCC). The IHC data were derived by the pathologists from triplicate cores

and include an estimate of the percentage (~ 100 cells) and intensity (on a scale of 0-3+) of cells that stained for a particular antigen under investigation. Where applicable, these two measures were combined to create a staining index for that particular biomarker by multiplying the intensity (0 to 3) by the percentage of cells in that category, resulting in a scale from 0 to 300. A staining index was calculated for AR, CK14, cyclin D1, PSA, PSMA, p27 and Her2/neu,.CD34 was evaluated by the percentage of positive endothelial cells in a specific tissue compartments (i.e. benign intervening stroma, stroma that is adjacent to tumor, stroma adjacent to PIN etc), Ki67, was evaluated based on percentage of positive cells in each of the intensity category and the remaining CK18, CD45, CD68 were assessed for percentage of positive cells at a single 3+ intensity.

Table 8. Antibodies used for immunohistochemistry

Biomarker	Antibody
Ki-67	Clone ki-67 (DAKO)
Cytokeratin 18	Clone DC-10 (Novocastra)
CD45	Clone X16/99
CD68	Clone 514H2 (Novocastra UK)
CD34	Clone QBEnd 101 (DAKO)
AR	Clone AR27 (Novocastra)
Cytokeratin 14	Clone LL002 (Novocastra)
Cyclin D1	Clone P2D11F11
PSA	Clone PA05 (Neomarkers)
PSMA	Clone ZMD.80 (Zymed)[P]
$p27^{Kip1}$	Clone DCS72 (Oncogene)
Her-2/neu	KIT DAKO[P]

[P] polyclonal; the remaining antibodies are monoclonal

Quantitative Immunofluorescence

Tissue microarray tissue samples were deparaffinized and rehydrated per standard procedures. Antigen retrieval was performed by boiling the slides in a microwave oven for 7.5 minutes in 1X Reveal solution (BioCare Medical, Walnut Creek, CA). The slides

were allowed to cool for 20 minutes at room temperature and then were washed twice for three minutes in phosphate-buffered saline (PBS).

The tissue samples underwent the following pre-antibody treatment steps. To help permeate the cellular structures of the tissue, the samples were incubated in PBS containing 0.2% Triton-X 100 (PBT) at room temperature for thirty minutes, followed by three rinses of three minutes each in PBS. To help reduce auto-fluorescence in the tissue, the samples were incubated in 1% HCl in 70% ethanol at room temperature for twenty minutes, followed by three rinses of three minutes each in PBS. Blocking of non-specific binding sites was performed by incubating the slides in 1% Blocking Reagent (10.0 mg/ml BSA in PBS) at room temperature for twenty minutes. No washes were performed between the blocking step and the subsequent hybridization step.

A cocktail of anti-cytokeratin 18 (CK18) antibody (Calbiochem) diluted at 1:7000 and androgen receptor (AR) antibody (clone AR441, LabVision) diluted at 1:5 dilution was made in 1% Blocking Reagent. Approximately 100 µl of this antibody cocktail was applied to the tissue sample, and the antibodies and tissue samples were allowed to hybridize in a humid chamber at room temperature for one hour. Hybridization was followed by two rinses of six minutes each in PBT, one rinse of six minutes in PBS, and one rinse of three minutes in PBS.

For the labeling step, a cocktail of Zenon Alexa Fluor 488 anti- Rabbit IgG Fab fragment and Zenon Alexa Fluor 568 anti-mouse IgG1 Fab fragment (Invitrogen, Carlsbad, CA)

was made in 1% Blocking Reagent at twice the concentrations recommended by the manufacturer (1:50 dilution for each Fab fragment). Approximately 100 µl of this labeling cocktail was applied to the tissue samples, which were then incubated in a humid chamber at room temperature for 30 minutes. The labeling reaction was followed by two rinses of six minutes each in PBT, one rinse of six minutes in PBS, and one rinse of three minutes in PBS.

We have also been able to evaluate 5 antibodies in a single prostate section using the following protocol: A cocktail of anti-racemase (AMACR; clone 13H4, Zeta Corporation) at a 1:50 dilution was made with undiluted antibody against high molecular weight cytokeratin + p63 (HMW CK + p63; BioCare Medical). Approximately 100 µl of this antibody cocktail was applied to the tissue sample, and the antibodies were allowed to bind in a humid chamber at room temperature for one hour. Incubation was followed by two rinses of six minutes each in PBT, one rinse of six minutes in PBS, and one rinse of three minutes in PBS.

For the labeling step, a cocktail of Zenon Alexa Fluor 488 anti-Rabbit, IgG Fab fragment Zenon Alexa Fluor 555 anti-mouse IgG1 Fab fragment, and Zenon Alexa Fluor 594 anti-mouse IgG2a Fab fragment was made in 1% Blocking Reagent at twice the concentrations recommended by the manufacturer (1:50 dilution for each Fab fragment). Approximately 100 µl of this labeling cocktail was applied to the tissue samples, and the tissue samples were incubated in a humid chamber at room temperature for 30 minutes.

The labeling reaction was followed by two rinses of six minutes each in PBT, one rinse of six minutes in PBS, and one rinse of three minutes in PBS.

The tissue samples were then treated to a second round of antibody binding and labeling. A cocktail of anti-CK-18 at a 1:6000 dilution and anti-AR at a 1:5 dilution was made in 1% Blocking Reagent. Approximately 100 µl of this antibody cocktail was applied to the tissue sample, and the antibodies were allowed to bind in a humid chamber at room temperature for one hour. Hybridization was followed by two rinses of six minutes each in PBT, one rinse of six minutes in PBS, and one rinse of three minutes in PBS.

For the second labeling step, a cocktail of Zenon Alexa Fluor 647 anti-Rabbit IgG Fab fragment and Zenon Alexa Fluor 568 anti-mouse IgG1 Fab fragment was made in 1% Blocking Reagent at the concentration recommended by the manufacturer (1:100 dilution for each Fab fragment). Approximately 100 µl of this labeling cocktail was applied to the tissue samples, and the tissue samples were incubated and rinsed as described for the first labeling step. The results are shown in the figure below.

Five antibodies on a single prostate tissue section

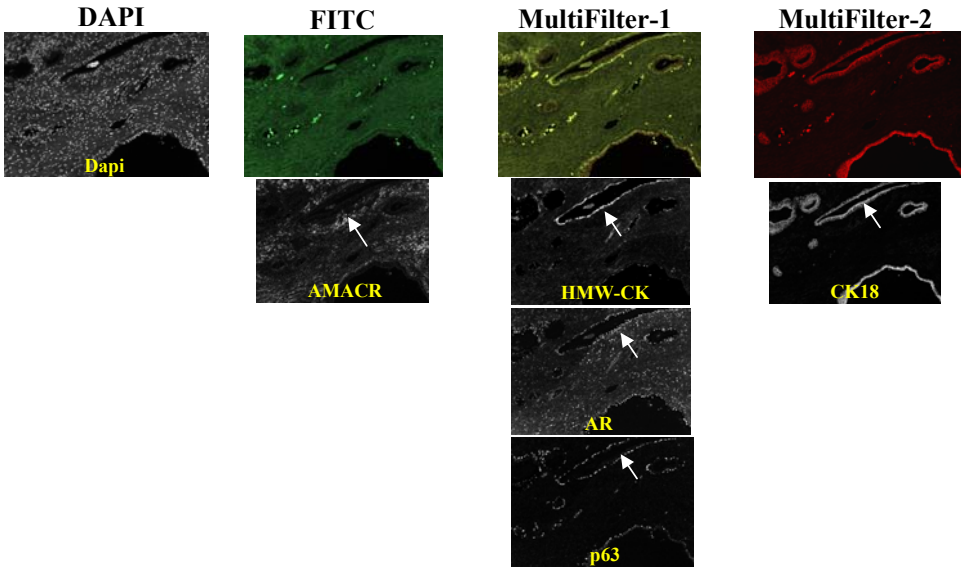

In all immunofluorescence experiments, samples were fixed by incubation in 10% formalin at room temperature for 10 minutes, followed by two rinses of three minutes each in PBS. SlowFade Light Antifade equilibration buffer (Invitrogen) was added to cover the tissue section, and this was incubated at room temperature for two minutes. The SlowFade Light equilibration buffer was removed from the sample, and approximately 100 µl of SlowFade Light Antifade with DAPI mounting solution was applied to the samples, which were then cover slipped. Samples were stored at -20ºC until analysis could be performed.

Image Acquisition

Fluorescent TMA images were acquired using a CRI Nuance multispectral camera (Cambridge Research & Instrumentation, Inc.) mounted on a Nikon 90i automated fluorescence microscope and controlled by MetaMorph online software. 12-bit DAPI images were captured with the camera set at 480 nm using a 50% saturation setting. Images of CK18, labeled with Alexa 488, were acquired using a FITC bandpass filter (Chroma). Five 12-bit images in 10 nm increments where captured starting at 520 nm. AR, labeled with Alexa 568, was captured using a custom-made longpass filter (Chroma). Eleven 12-bit images in 10 nm increments where captured starting at 570 nm. Image stacks were unmixed using the CRI analysis software. Pure Alexa 488 and 568 dye were used as reference spectra for the unmixing process. Typical regions of autofluorescence and other fluorescent objects (e.g. erythocytes) were assigned to spectral profiles in order to complete the spectral library. After completion of the unmixing process, quantitative gray-scale tiff images where stored for the analysis.

Image Analysis for quantitation of AR

The high resolution gray-scale tiff images (1280 x 1024 pixels) were individually processed with an object-oriented algorithm which identified the area and intensity level for AR within epithelial and stromal nuclei in TMA cores. We did not discriminate between tumor and normal elements, only between stromal and epithelial cells; CK18 expression served as the topographical marker for all prostate epithelial cells. The script overlayed the individual 'morphologic' layers, i.e. DAPI for nuclei, CK18 for epithelial cells and AR, and, by employing discrete Alexa fluorochromes and pre-established thresholds to remove background and non-specific binding, was able to accurately define

AR intensity. The analysis equates protein concentration to absolute positive pixel counts with individual features reflecting a series of morphologic correlates, including nuclear (DAPI-stained) area occupied by AR and the relative amount of AR protein present within epithelial and stromal nuclei. AMACR positive epithelial cells were used as an additional descriptor for AR content and derived features were assessed as part of the overall model development.

Analytical and Statistical Results

In the SVRc Feature Reduction algorithm employed in the original study, an initial SVRc model is constructed using all the features in the cohort. This model is then tested on the training cohort and a fitness criterion (described below) is assessed. All the features in the model are ranked in order of the absolute value of their contribution (the product of feature weight and variance; negative contributions imply negative correlation with time-to-recurrence). The feature with the lowest contribution to the model is dropped and a new model is constructed on the remaining features. This procedure is repeated until there are no more features left for a SVRc model to be trained on. At this point, the model with the highest fitness is selected. In the case of multiple models with equal values of the fitness, the model with the fewest features is selected. Consequently, all the features in the final model are essential for maintaining predictive accuracy. Even removing the feature with the least prognostic contribution to the final model results in a loss of predictive accuracy.

In this manner, the optimized model is computed leveraging the inherent capabilities of support vector machines with a linear kernel to estimate the input of each feature in the model. By removing features with low weights that do not add valuable information, the model is simplified and may be improved, since these features may in fact be adding noise.

The fitness criterion used to assess each intermediate model during the feature reduction process was a combination of the three evaluation metrics currently employed at Aureon: concordance index, sensitivity, and specificity.

The final PSA recurrence model constructed with the SVRc Feature Reduction algorithm consists of eight prognostic variables. These variables and their relative weights within the model are listed above in Table 1. A negative weight indicates that the presence of each feature (or higher value of a continuous feature) was associated with a shorter time to PSA recurrence, whereas a positive weight indicates the opposite. These weights illustrate the respective contribution of each variable in the complete model. A Kaplan-Meier curve of freedom from PSA recurrence within 5 years according to SVRc validation model score is illustrated in Figure 3b. Patients were stratified into low and high risk groups based on the sensitivity/specificity cut point. Red circles indicate events.

In the expanded study, an alternative feature selection method also developed for SVRc was employed. In this SVRc Bootstrap Feature Selection algorithm, an initial filtering step removes features that do not univariately correlate with the outcome of interest.

Next, N different splits (in this study, N=25) are made of the training data; in each split approximately two-thirds of that total training instances are randomly assigned to a training subset and approximately one-third of the total training instances are randomly assigned to a testing subset.

The algorithm begins with a "greedy-forward" feature selection process starting with all the features that passed the initial filter. For each feature, N models are built on the training subsets across all the splits, and validated on the N respective testing subsets. The overall performance for each feature is averaged across the N runs. The feature with the best overall performance is selected. In the next step, each feature is added to the previously selected feature(s) and again N models are built and tested across the splits. The feature whose addition resulted in the best overall performance is selected. The algorithm continues in this fashion until there are no more features that will improve the performance.

Subsequently, a "greedy-backward" feature selection approach is employed. Each feature is removed, and N models without that feature across the splits are built and tested. The feature whose removal results in the best overall performance is removed, and the procedure is repeated until the model performance ceases to improve due to the removal of features. This step reduces model complexity and removes features that may have initially been significant, but their information contribution is encapsulated within a feature added subsequently.

Finally, the complete SVRc model is trained using all the selected features on the complete training data.

The final extended PSA recurrence model constructed with the SVRc Bootstrap Feature Selection algorithm also consists of eight prognostic variables. These variables and their relative weights within the extended model are listed below in Supplementary Table 9. A negative weight indicates that the presence of each feature (or higher value of a continuous feature) was associated with a shorter time to PSA recurrence, whereas a positive weight indicates the opposite. These weights illustrate the respective contribution of each variable in the complete model. A Kaplan-Meier curve of freedom from PSA recurrence within 5 years according to SVRc training model score is illustrated in Supplemenrary Figure 1. Patients were stratified into low and high risk groups based on the sensitivity/specificity cut point.

Table 9. Extended PSA recurrence model with prognostic variables and their relative weight.

Feature	Relative Weight in Model
Biopsy Gleason Sum	-25.60
Seminal vesicle invasion	-22.69
Extracapsular extension	-4.37
PSA	-13.81
Relative Area of AR+ epithelial nuclei	-10.64
Texture of tumor epithelial nuclei	-19.21
Texture of tumor epithelial cytoplasm	18.19
Dominant Prostatectomy Gleason grade	-10.93

Figure 1. Kaplan-Meier curve of the extended PSA Recurrence model. Confidence intervals are illustrated on the graph.